Efficiency of a Propulsor on a Body of Revolution-Inducting Boundary-Layer Fluid

S. THURSTON* AND M. S. EVANBAR†
Northrop Corp., Hawthorne, Calif.

The energy relationships that define the efficiency of propulsors that induct boundary-layer fluid on a body of revolution have been derived, and the quantitative interrelationships of associated parameters have been developed. The results illustrate that an increase in the jet efficiency of up to 25% over the freestream propulsor is attainable by proper selection of design parameters. It is further demonstrated that jet efficiency values of well over 100% are attainable; the theoretical maximum is 200%. As a result, values of propulsive efficiency approaching 100% are attainable using modern state-of-art propellers or pumpjets. The shape of modern torpedoes and submarines closely approximates a body of revolution; this forms the basis for the present analysis.

Nomenclature

η_{jet} = jet or ideal efficiency
η_{hyd} = hydraulic efficiency
η_{prop} = propeller efficiency
η_{propul} = propulsive efficiency
shp = shaft horsepower
D = drag
T = thrust
τ = thrust deduction factor
r = radial distance from body surface
n = exponential constant
δ = boundary-layer thickness
δ_1 = boundary-layer thickness at station 1
δ_p = boundary-layer thickness inducted into the propulsor
δ_j = boundary-layer thickness at station j
V = boundary-layer velocity
V_δ = local stream velocity
V_0 = freestream velocity
V_1 = boundary-layer velocity at station 1
V_j = boundary-layer velocity at station j
p = static pressure
P = total pressure
D_t = total drag
D_f = drag resulting from inducted boundary-layer fluid
D_0 = drag other than D_f
C = D_t/D_f
m = momentum of boundary-layer fluid
ξ = δ_p/δ
ρ_0 = mean weight density of sea water
W_p = flow rate inducted into propulsor, lbs/sec
g = acceleration of gravity
K = $V_j - V_1$, propulsor loading parameter
E_p = energy added to the flow by the propulsor

Introduction

VISCOUS flow over a self-propelled body of revolution is a complex phenomenon. The development of a boundary-layer over the body shown in Fig. 1 is accompanied by skin friction drag, modified flow parameters, and pressure drag. If the propulsor is located sufficiently distant from the boundary-layer, it will induct freestream fluid and not cause any change in the boundary-layer itself. Examples are an airship or submarine, self-propelled by outboard fin-mounted propellers. On the other hand, if the propulsor is immersed in the boundary layer, a change in the flow field upstream of the propulsor will be induced, altering the pressure and the velocity distribution and also the drag of the body. Consequently, a body propelled by an aft-mounted propulsor, coaxial with the body centerline, inducting boundary-layer flow represents a much more complicated flow problem than a body propelled by a propulsor inducting freestream flow. Examples are single-screw submarines and torpedoes. However, with the more complex flow picture, the boundary-layer propulsor offers significant performance improvements over the freestream case and merits serious attention.

It has been known for many years that a propeller or pumpjet, inducting a wake or immersed in a boundary-layer, can recover some of the lost energy that is reflected in the momentum decrement, with a resultant increase in the propulsive efficiency. However, there has not been a systematic analysis to quantify the extent of potential improvement in propulsive efficiency that can be attained by proper control of the design parameters. There has not been a serious effort to design a propulsor for the maximum attainable efficiency, even though substantial improvements in efficiency are possible.

The intent herein is to develop analytically the energy relationships that define the propulsive efficiency for a submerged body of revolution and the quantitative interrelationships of associated parameters on a systematic basis. In addition, the gains or improvements in the jet, or ideal efficiency that can be attained by a propulsor inducting boundary-layer fluid, are determined. The theoretical maximum attainable efficiency then is determined. The equivalent relationships for the freestream case with uniform inflow are derived and shown to be a specialized case of the foregoing.

Efficiency of Propulsion of a Self-Propelled Body

As a basis for the evaluation of propulsive systems for marine craft, defining the energy relations that act on a self-propelled body, and the resulting efficiency interrelationships, is of particular interest.

When the propulsor inducts boundary-layer fluid, the induced effects of the propulsor change the pressure and velocity distributions on the body in the region of the propulsor, with a consequent effect on the drag. In order to propel the body, the propulsor therefore must supply a thrust equal to this modified drag. This can be greater or less than the tow rope drag:

$$T = \text{tow rope drag} + \Delta\text{drag} = D(1 + \tau)$$

The incremental thrust required to compensate for the Δ drag is referred to as "thrust deduction." This term is usually positive in that it acts to increase the drag of the body in the case of a conventional free propeller; however, in certain specific cases, it can be zero or possibly negative. Therefore,

Presented as Preprint 65-234 at the AIAA/USN Marine Systems & ASW Conference, San Diego, Calif., March 8–10, 1965; submitted July 2, 1965; revision received December 8, 1965.

* Chief, Advanced Underwater Systems Group, Norair Division. Member AIAA.
† Engineer, Advanced Underwater Systems Group, Norair Division.

thrust deduction must be included in evaluating the efficiency of propulsion, which is

$$\eta_{propul} = \text{output/input} = DV_0/\text{shp} = TV_0/(1 + \tau)\ \text{shp}$$

where T represents the thrust that must be supplied for the body to be self-propelled at velocity V_0.

Another efficiency can be defined, based on the thrust output of the propeller, as $\eta_{prop} = TV_0/\text{shp}$. This is related to η_{propul} by $\eta_{propul} = \eta_{prop}/(1 + \tau)$. For the freestream case, where $\tau = 0$, $\eta_{propul} = \eta_{prop}$.

The foregoing efficiencies must be used with caution, because they are relationships of energies and not efficiencies in the absolute sense. The propeller efficiency alternately has been referred to as a figure of merit.[1]

The propeller efficiency defines the ratio of thrust power to shaft power. This process actually consists of the following steps.

1) The shaft power provided by the prime mover is converted to hydraulic power or kinetic energy in the water by the propulsor. The efficiency of this process can be termed a hydraulic efficiency: η_{hyd} = hydraulic power added to flow/shaft power.

2) The hydraulic power or kinetic energy added to the water by the propulsor then is converted to thrust power to overcome the drag of the body. The relationship of the thrust power to the hydraulic power is called the jet or ideal efficiency: η_{jet} = thrust power/hydraulic power added to flow.

The propeller efficiency then is

$$\eta_{prop} = \text{output/input} = \text{thrust power/shp} = \eta_{hyd} \times \eta_{jet}$$

If an ideal propulsor is used, $\eta_{hyd} = 100\%$ and $\tau = 0$. Then $\eta_{propul} = \eta_{prop} = \eta_{jet}$. Therefore, η_{jet} often is called the jet or ideal efficiency.

Differences between an Ideal and Practical Propulsor

The analysis presented herein considers an ideal propulsor or actuator disk. Although it is beyond the scope of this paper to consider all the factors which act on a propulsor, a brief discussion of some of these factors is merited.

Thrust Deduction

A conventional free propeller, operating in a wake or inducting boundary-layer fluid, will cause induced effects with a subsequent thrust deduction. Recent experiments substantiated by theoretical analysis[1, 2] have demonstrated that ventilating the base of the propeller can eliminate this thrust deduction penalty for specific operating conditions. In the case of the pumpjet, the resolution of forces becomes considerably more complex because of the shroud, and the thrust deduction factor acting on the system cannot be defined simply.

Rotational Losses

A propulsor that consists of a single rotating blade row (either a single free propeller or a shrouded propeller or pumpjet with a single rotor) produces rotational velocities in the wake as well as axial components that produce thrust. The thrust is the axial momentum rate of change produced by the propulsor, whereas the rotational components contribute to losses.

In order to minimize or eliminate these rotational losses, several approaches can be used. The following approaches apply to either the free propeller or shrouded propeller (pumpjet).

1) Vanes can be located upstream of the rotating blade row to prewhirl the flow against the direction of rotor rotation. The flow is straightened then by the rotating blades as they add energy, so that the flow exits axially.

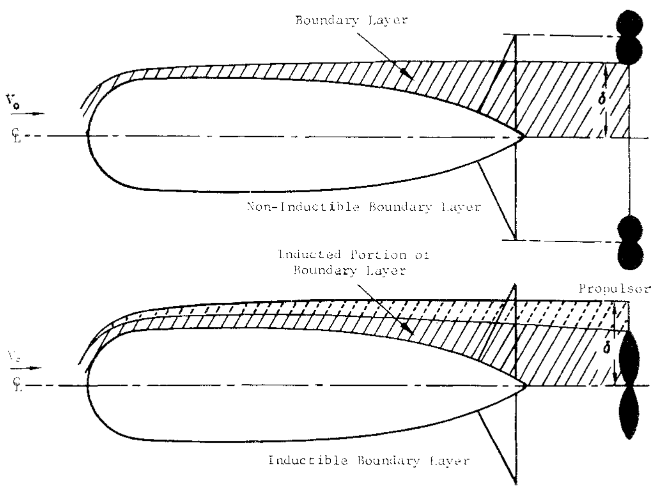

Fig. 1 Schematic of boundary layer on a body of revolution.

2) Straightening vanes can be located downstream of the rotating blade row to remove the whirl.

3) Counterrotating blade rows can be utilized whereby the whirl components imparted by the forward propeller are removed by the aft propeller.

Propulsor Loading Distribution

When a propulsor inducts boundary-layer fluid on the afterbody of revolution (e.g., a torpedo), recovery of a portion of the kinetic energy of the wake of the body is possible. If the wake is completely and uniformly filled, the wake energy losses will be at a minimum. However, this is impractical because of several factors.

For a free propeller, the loading must go to zero at the blade tips. Also, as the flow velocity theoretically goes to zero at the hub, the amount of energy which can be added in the hub region is limited. A pumpjet is not subject to the same limitations at the tip (due to the effect of the shroud), although the conditions are similar at the hub. Loading distributions are restricted further by cavitation limitations.

Some typical circulation distributions used in propeller design and the resulting propeller efficiencies are examined in Ref. 3. For the distributions used, the effects on efficiency are small; a variation of only 3% was obtained over most of the range.

In order to provide some insight into the influence of loading or circulation distribution on jet efficiency, the analysis considered two cases: 1) a uniformly filled wake with a constant jet velocity, which represents a limiting condition; and 2) a velocity profile exiting from the propulsor (similar to the inflow), with the propulsor adding a constant ΔV. This constant ΔV distribution has been used for preliminary design studies of pumpjets and is a convenient parameter for analysis.

Case I: General Analysis—Jet Efficiency

Conditions and Assumptions

Consider a body of revolution (Fig. 2) operating at a forward velocity (V_0) sufficiently beneath the water surface so that there is no wave drag. The body is at zero angle of attack and the flow follows symmetrical annular stream tubes about the body. The flow is fully turbulent and the boundary layer follows the classical turbulent laws as it progresses downstream along the body.

It is a reasonable approximation to express the boundary-layer velocity profile, at any point along the body upstream of the propulsor, as

$$V = V_\delta (r/\delta)^{1/n} \quad (1)$$

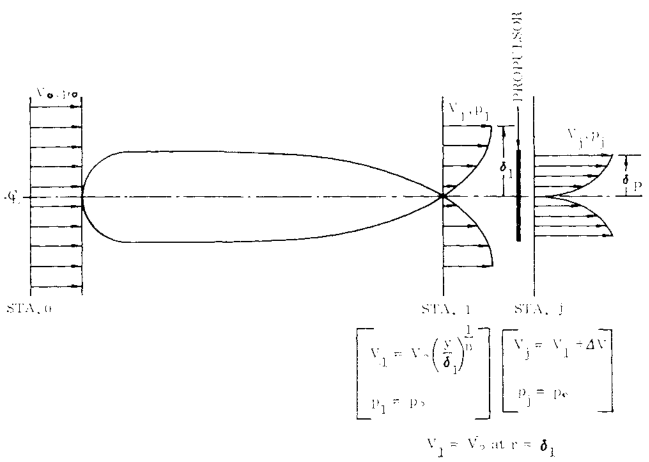

Fig. 2 Schematic of body of revolution—control stations noted.

At station 1, it is assumed that $p_1 = p_0$, $V_\delta = V_0$ and; at station j, $p_j = p_0$.

An ideal propulsor or actuator disk is located at the trailing edge of the body. It is assumed that there are no losses within the propulsor or in the exiting flow, and no induced effects are present. The propulsor adds energy to the flow such that $V_j - V_1$ is constant along each stream tube.

Drag

The total drag of the body can be represented by two parameters: $D_{\text{total}} = D_{\text{friction}} + D_{\text{other}}$. The first term ($D_f$) is the friction drag of the flow over the body and is represented by the cumulative momentum decrement in the boundary layer entering the propulsor at station 1. However, D_f may also include any form drag resulting from skin friction upstream of the propulsor. As the flow is axisymmetric, the entire boundary layer can be inducted into a propulsor of proper design. The second term (D_0) includes the portion of the drag due to other extraneous sources not represented in the boundary-layer flow entering the propulsor (such as drag due to appendages, fins, and/or control surfaces, and body form drag occurring downstream of the propulsor). This drag is not inductible into the propulsor. In the case of the pumpjet, the noninductible drag can also include the friction drag of the outer surface of the shroud. In a well-designed underwater body, the friction drag can account for 80 to 90% of the total drag. The total drag can be expressed conveniently as

$$D_{\text{total}} = C \times D_{\text{friction}} \tag{2}$$

where $C \geqq 1$. D_{total} represents the total tow rope drag.

At station 1, the momentum flux in the boundary layer is defined by

$$m_1 = \frac{2\pi\rho_0}{g}\left[\int_0^{r=\delta_1} (rV_1)V_1 dr\right] \tag{3}$$

The friction drag is represented by the rate of change in axial momentum flux between stations 0 and 1:

$$D_f = \frac{2\pi\rho_0}{g}\left[\int_0^{r=\delta_1} (rV_1)(V_0 - V_1)dr\right] \tag{4}$$

$$D_f = \frac{2\pi\rho_0}{g}\left[\left(\int_0^{r=\delta_1} rV_1V_0 - \int_0^{r=\delta_1} rV_1^2\right) dr\right]$$

From Eq. (1),

$$V_1 = V_{\delta_1}(r/\delta_1)^{1/n} \text{ and, } V_{\delta_1} = V_0$$

Substituting,

$$D_f = \frac{2\pi\rho_0}{g}\left[\int_0^{r=\delta_1} rV_0^2\left(\frac{r}{\delta_1}\right)^{1/n} dr - \int_0^{r=\delta_1} rV_0^2\left(\frac{r}{\delta_1}\right)^{2/n} dr\right]$$

$$D_f = \frac{V_0^2(2\pi\rho_0)}{g}\left[\int_0^{r/\delta_1=1} r\delta_1\left(\frac{r}{\delta_1}\right)^{1/n} \times d\left(\frac{r}{\delta_1}\right) - \int_0^{r/\delta_1=1} r\delta_1\left(\frac{r}{\delta_1}\right)^{2/n} d\left(\frac{r}{\delta_1}\right)\right]$$

Integrating and simplifying,

$$D_f = \frac{2\pi\rho_0V_0^2}{g}\left[\delta_1^2\int_0^1\left(\frac{r}{\delta_1}\right)^{1+1/n} d\left(\frac{r}{\delta_1}\right) - \delta_1^2\int_0^1\left(\frac{r}{\delta_1}\right)^{1+2/n} d\left(\frac{r}{\delta_1}\right)\right]$$

$$D_f = \frac{2\pi\rho_0V_0^2\delta_1^2}{g}\left[\frac{1}{2+1/n} - \frac{1}{2+2/n}\right]$$

The friction drag is

$$D_f = (\pi\rho_0V_0^2\delta_1^2/g)[n/(2n+1)(n+1)] \tag{5}$$

The total drag is, therefore,

$$D_t = D_fC = (\pi\rho_0V_0^2\delta_1^2/g)[n/(2n+1)(n+1)]C \tag{6}$$

Thrust

Thrust is the rate of change in axial momentum flux through the propulsor. The momentum flux at station j is

$$m_j = \frac{2\pi\rho_0}{g}\left[\int_0^{\delta_1\xi} (rV_1)V_j dr\right] \tag{7}$$

where $\xi \leqq 1$ and represents the portion of the boundary layer inducted by the propulsor. The momentum flux at station 1 is given by

$$\left.\begin{aligned} m_1 &= \frac{2\pi\rho_0}{g}\left[\int_0^{\delta_1\xi} rV_1^2 dr\right] \\ T = m_j - m_1 &= \frac{2\pi\rho_0}{g}\left[\int_0^{\delta_1\xi} (rV_1V_j - rV_1^2)dr\right] \\ &= \frac{2\pi\rho_0}{g}\left[\int_0^{\delta_1\xi} rV_1(V_j - V_1)dr\right] \end{aligned}\right\} \tag{8}$$

When $\xi = 1$, the total momentum decrement represented in the boundary layer is inducted into the propulsor. Station is located at a point where $P_j = P_0$. For this analysis, the propulsor adds energy to the flow, such that $(V_j - V_1)$ is constant along each stream tube:

$$K = V_j - V_1 \qquad V_j = K + V_1 \qquad V_1 = V_0(r/\delta_1)^{1/n}$$

Substituting and simplifying,

$$T = \frac{2\pi\rho_0}{g}\left[\int_0^{\delta_1\xi} rV_1(K + V_1 - V_1)dr\right]$$

$$= \frac{2\pi_0V_0K}{g}\left[\int_0^{\delta_1\xi} r\left(\frac{r}{\delta_1}\right)^{1/n} dr\right]$$

$$= \frac{2\pi\rho_0V_0K\delta_1^2}{g}\left[\int_0^{\xi}\left(\frac{r}{\delta_1}\right)^{1+1/n} d\left(\frac{r}{\delta_1}\right)\right]$$

Integrating, the thrust is

$$T = (2\pi\rho_0KV_0\delta_1^2n/g)[(\xi)^{2+1/n}/(2n+1)] \tag{9}$$

Dynamic Equilibrium

For the body to be in dynamic equilibrium at a forward velocity (V_0), the thrust must equal the drag. If there are no induced effects and/or propulsor-body interactions, the thrust required is equal to the tow rope drag of the body:

$$\frac{2\pi\rho_0 K V_0 \delta_1^2 n}{g}\left[\frac{(\xi)^{2+1/n}}{2n+1}\right] = \left[\frac{\pi\rho_0 V_0^2\delta_1^2}{g}\right]\frac{n}{(2n+1)(n+1)}C \tag{10}$$

Simplifying and solving for K,

$$\left.\begin{aligned} 2K(\xi)^{2+1/n} &= [V_0/(n+1)]C \\ K &= [(V_0C)/2(n+1)][1/(\xi)^{2+1/n}] \\ K &= [V_0/2(n+1)(\xi)^{2+1/n}]C \end{aligned}\right\} \tag{11}$$

The jet velocity is therefore

$$V_j = (V_0C)/2(n+1)(\xi)^{2+1/n} + V_0(r/\delta_1)^{1/n} \tag{12}$$

Energy Added by Propulsor

The energy added to the flow by the propulsor is

$$E_p = \frac{\pi\rho_0}{g}\left[\int_0^{\delta_1\xi} rV_1(V_j^2 - V_1^2)dr\right] \tag{13}$$

As $V_j - V_1 = K$, $V_j^2 = K^2 + 2KV_1 + V_1^2$ and

$$E_p = \frac{\pi\rho_0}{g}\left[\int_0^{\delta_1\xi} rV_1K^2dr + \int_0^{\delta_1\xi} 2rKV_1^2dr\right] \tag{14}$$

$$E_p = \frac{K\pi\rho_0}{g}\left[\int_0^{\delta_1\xi} KrV_0\left(\frac{r}{\delta_1}\right)^{1/n} dr + \int_0^{\delta_1\xi} 2rV_0^2 \times \left(\frac{r}{\delta_1}\right)^{2/n} dr\right] = \frac{V_0K\pi\rho_0}{g}\left[\delta_1^2K\int_0^{\delta}\left(\frac{r}{\delta_1}\right)^{1+1/n} \times d\left(\frac{r}{\delta_1}\right) + 2V_0\delta_1^2\int_0^{\delta}\left(\frac{r}{\delta_1}\right)^{1+2/n} d\left(\frac{r}{\delta_1}\right)\right]$$

Integrating,

$$\begin{aligned} E_p &= \frac{V_0K\pi\rho_0\delta_1^2}{g}\left[\frac{K(\xi)^{2+1/n}}{2+1/n} + \frac{2V_0(\xi)^{2+2/n}}{2+2/n}\right] \\ &= \frac{V_0K\pi\rho_0\delta_1^2 n(\xi)^{2+1/n}}{g}\left[\frac{K}{2n+1} + \frac{V_0(\xi)^{1/n}}{1+n}\right] \end{aligned} \tag{15}$$

Jet Efficiency

The jet efficiency is

$$\eta_{\text{jet}} = \text{thrust power/hydraulic power} = TV_0/E_p \tag{16}$$

Substituting,

$$\begin{aligned} \eta_{\text{jet}} &= 2V_0(1+n)/[K(1+n) + V_0(2n+1)(\xi)^{1/n}] \\ &= 2(1+n)/[(K/V_0)(1+n) + (2n+1)(\xi)^{1/n}] \end{aligned} \tag{17}$$

Substituting,

$$\begin{aligned} K &= CV_0/2(n+1)(\xi)^{2+1/n} \\ \eta_{\text{jet}} &= \frac{2V_0(1+n)}{CV_0/2(\xi)^{2+1/n} + V_0(2n+1)(\xi)^{1/n}} \end{aligned} \tag{18}$$

The jet efficiency is therefore

$$\eta_{\text{jet}} = \frac{2(1+n)}{C/2(\xi)^{2+1/n} + (2n+1)(\xi)^{1/n}} \tag{19}$$

Maximum Jet Efficiency

Determining the parametric interrelations for the maximum efficiency is of interest. To maximize η_{jet} as a function of ξ, set

$$\partial(\eta_{\text{jet}})/\partial(\xi) = 0$$

$$\frac{\partial(\eta_{\text{jet}})}{\partial(\xi)} = -2(1+n) \times \frac{\dfrac{[-(4+2/n)C(\xi)^{1+1/n} + [(2n+1)/n](\xi)^{(1/n)-1}]}{4(\xi)^{4+2/n}}}{\left[\dfrac{C}{2(\xi)^{2+1/n}} + (2n+1)(\xi)^{1/n}\right]^2} \tag{20}$$

Solving for ξ,

$$\left.\begin{aligned} \frac{2n+1}{n}(\xi)^{(1/n)-1} &= \frac{(4+2/n)C(\xi)^{1+1/n}}{4(\xi)^{4+2/n}} \\ \left(2+\frac{1}{n}\right)\frac{(\xi)^{1/n}}{\xi} &= \frac{2(2+1/n)C(\xi)\xi^{1/n}}{4(\xi)^4(\xi)^{2/n}} \\ (\xi)^{2+2/n} = C/2 \qquad & \xi = (C/2)^{n/(2n+2)} \end{aligned}\right\} \tag{21}$$

Substituting ξ in

$$\left.\begin{aligned} \eta_{\text{jet}} &= \frac{2(1+n)}{C/2(\xi)^{2+1/n} + (2n+1)(\xi)^{1/n}} \\ \eta_{\text{jet}_{\max}} &= \frac{2(1+n)}{\dfrac{C}{2(C/2)^{(2n+1)/(2n+2)}} + (2n+1)\left(\dfrac{C}{2}\right)^{1/(2n+2)}} \\ \eta_{\text{jet}_{\max}} &= \frac{2(1+n)}{\dfrac{(C)^{1/(2n+2)}}{(2)^{1/(2n+2)}} + (2n+1)\left(\dfrac{C}{2}\right)^{1/(2n+2)}} \end{aligned}\right\} \tag{22}$$

$$\left.\begin{aligned} \eta_{\text{jet}_{\max}} &= \frac{2(1+n)}{(C/2)^{1/(2n+2)}[1+(2n+1)]} \\ &= \frac{1}{(C/2)^{1/(2n+2)}} \end{aligned}\right\} \tag{23}$$

The maximum jet efficiency is therefore

$$\eta_{\text{jet}_{\max}} = (2/C)^{1/(2n+2)} \tag{24}$$

Theoretical Maximum Attainable Jet Efficiency

The theoretical maximum attainable efficiency for a propulsor inducting boundary-layer fluid is a limiting value of considerable interest. For this case, consider that the entire boundary layer is inducted and that the flow is completely stopped at station 1. Therefore, the velocity at any radial point at station 1 is zero.

The theoretical maximum efficiency results when $V_j = V_0$. From Eq. (16),

$$\eta_{\text{jet}_{\max}} = TV_0/E_p = TV_j/E_p \tag{25}$$

The rate of change of momentum flux across the propulsor is

$$T = \frac{2\pi\rho_0}{g}\left[\int_0^{\delta_j} rV_j^2dr - \int_0^{\delta_1} rV_1^2dr\right] = \frac{\pi\rho_0\delta_j^2V_j^2}{g}$$

The rate of change of energy flux across the propulsor is

$$E_p = \frac{\pi\rho_0}{g}\left[\int_0^{\delta_j} rV_j^3dr - \int_0^{\delta_1} rV_1^3dr\right] = \frac{\pi\rho_0\delta_j^2V_j^3}{2g}$$

Substituting in Eq. (25),

$$\eta_{\text{jet}_{\max}} = 2 \tag{26}$$

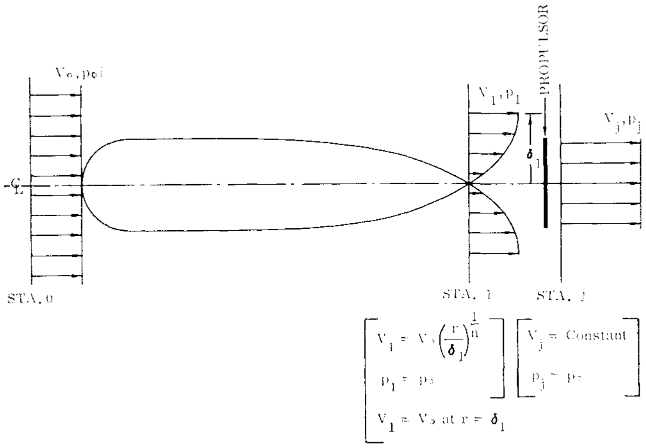

Fig. 3 Schematic of body of revolution—control stations noted.

Freestream Case

Consider the freestream case with uniform inflow. This case could correspond to propellers on a twin-screw submarine or a ship where the propeller is far beneath the hull. The flow approaches the propulsor with uniform velocity V_0 and leaves with uniform velocity V_j.

The propulsive efficiency relationship is derived readily from simple momentum considerations as follows. The thrust is

$$T = (W_p/g)(V_j - V_0) \tag{27}$$

The energy added to the water by the propulsor is

$$E_p = (W_p/2g)(V_j^2 - V_0^2) \tag{28}$$

The jet efficiency is

$$\eta_{\text{jet}} = \frac{TV_0}{E_p} = \frac{W_pV_0(V_j - V_0)}{g} \times \frac{2g}{W_p(V_j^2 - V_0^2)} = 2V_0/(V_j + V_0) \tag{29}$$

The freestream case also can be considered to be a simplified case I: $K = V_j - V_1$, where V_j and V_1 are both invariant. In the relation considered for the inflow velocity, the freestream case corresponds to

$$V_1 = V_0(r/\delta)^{1/n} \quad \text{as} \quad n \to \infty, \quad V_1 \to V_0$$

In this case, none of the skin friction drag is represented by a velocity decrement in the inflow to the propulsor, and considerations involving the boundary-layer are not needed.

From Eq. (17),

$$\eta_{\text{jet}} = 2V_0(1 + n)/[K(1 + n) + V_0(2n + 1)(\xi)^{1/n}] \tag{30}$$

Applying the limit process,

$$\eta_{\text{jet}} = \lim_{n\to\infty} \left[\frac{2V_0(1 + n)}{K(1 + n) + V_0(2n + 1)(\xi)^{1/n}}\right] = \frac{1}{K/2V_0 + 1} = 2V_0/(V_j + V_0) \tag{31}$$

Case II: General Analysis—Jet Efficiency

Conditions and Assumptions

This case differs from case I only in the loading distribution parameter added by the propulsor. It involves minimum energy losses in the wake where the wake is completely filled and V_j is a constant. All other conditions and assumptions remain the same. This case is illustrated by the schematic in Fig. 3.

The energy addition is $V_j - V_0(r/\delta_1)^{1/n}$. Employing the method of approach used in case I, the expressions relating jet efficiency to the parameters of interest were determined. The expression for the maximum jet efficiency was found to be

$$\eta_{\text{jet}_{\max}} = [(2n + 3)/2(n + 1)](C)^{-1/(2n+2)} \tag{32}$$

Discussion of Results

The foregoing analysis presents derivation of equations which define the jet or ideal efficiency of a propulsor inducting boundary-layer fluid. The effects of the pertinent performance and/or design parameters on the jet efficiency are evaluated in the following paragraphs.

Jet Efficiency with Constant ΔV Energy Addition

The calculated results for the case where the energy addition corresponds to a constant ΔV are shown in Figs. 4–6.

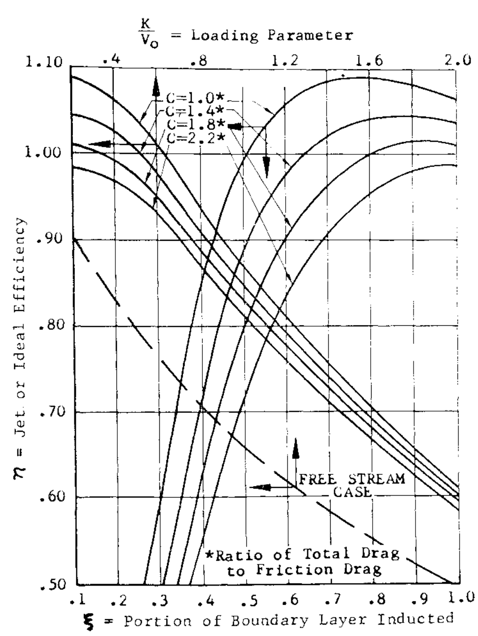

Fig. 4 Effects of performance parameters on ideal efficiency for a propulsor inducting the boundary layer on a body of revolution for $n = 3$.

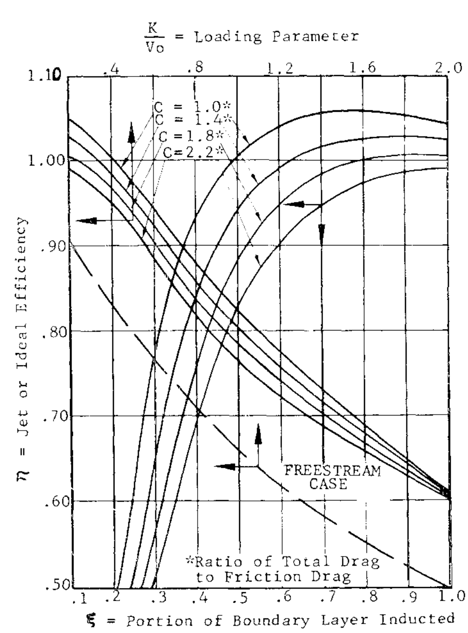

Fig. 5 Effects of performance parameters on ideal efficiency for a propulsor inducting the boundary layer on a body of revolution for $n = 5$.

The parameters represented are as follows:

C = the ratio of the total drag to the inductible friction drag
ξ = the portion of boundary layer inducted with respect to the total boundary-layer thickness
K/V_0 = the ΔV added by the propulsor as a proportion of V_0
n = the exponent which defines the exponential relationship of velocity in the turbulent velocity law
η_{jet} = jet or ideal efficiency

For any combination of parameters, the jet efficiency can be determined directly from the curves. It is more significant, perhaps, that the quantitative effect on the jet efficiency due to variation in any single parameter or combination of parameters can be determined.

The results demonstrate that the jet efficiency increases with the following: 1) increase in the amount of inductible drag, 2) decrease in the value of the exponent n, 3) decrease in the loading parameter, and 4) increase in the amount of boundary layer inducted up to approximately 70%. The last of these relationships depends on the type of energy addition. For the case where the jet velocity is uniform, the jet efficiency is maximum when the amount of boundary layer inducted is maximized.

A significant result is that the jet efficiency exceeds 100% over a wide region of the curves. This is illustrated more effectively in Fig. 7 which shows the maximum jet efficiency as a function of the exponent n for various values of C. These results were derived from Eq. (24) and represent jet efficiencies of 0.70 or greater. It is of interest that even for cases where C is approximately 2, which corresponds to a value of inductible friction drag equal to only $\frac{1}{2}$ of the total drag, the maximum jet efficiency is in the region of 100% or greater. The theoretical maximum attainable efficiency derived in Eq. (26) is 200%, which corresponds to the case where the flow is completely stopped in front of the propulsor and then accelerated to freestream velocity.

It is also of interest to compare the jet efficiency which can be attained when inducting boundary-layer fluid with that of the freestream inflow case for the same loading parameters.

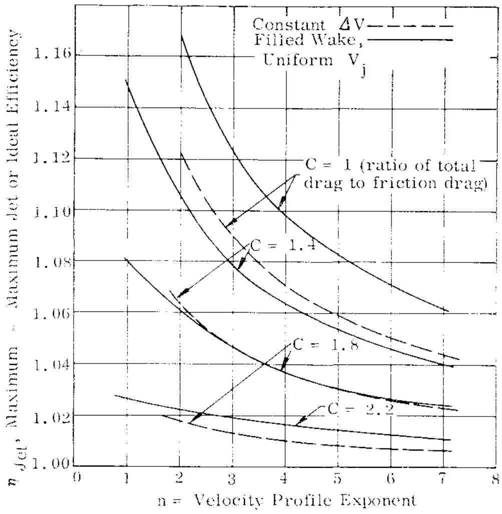

Fig. 7 Effects of performance parameters on the maximum ideal efficiency for a propulsor inducting the boundary layer on a body of revolution.

The theoretical maximum efficiency attainable with freestream inflow is 100%, which corresponds to the limiting case where the flow enters and leaves the propulsor with velocity V_0; there is no energy added by the propulsor. For any case of practical interest, the efficiency is less. For a loading parameter $K/V_0 = 0.2$, the maximum jet efficiency is reduced to 0.91 and further reduced to 0.79 when $K/V_0 = 0.5$. The jet efficiency for the boundary layer propulsor is significantly better. An increase of approximately 15% for exponent $n = 7$ and 23 to 25% for exponent $n = 3$ results over almost the entire range of loading parameters. The reasons for using a boundary-layer propulsor are clearly evident.

Figures 7–9 display the parametric interrelationships for a propulsor, inducting boundary-layer fluid where the energy addition is now $V_j - V_0(r/\delta_1)^{1/n}$ and the jet velocity is uniform. The same trends as discussed in case I are demonstrated; however, in this case the efficiency becomes maximum when the entire boundary-layer is inducted for all parameters. For this case, the energy added to the fluid by the propulsor varied exponentially across the boundary layer. Hence, a simple loading parameter could not be defined. However, the added complexity did not detract from the

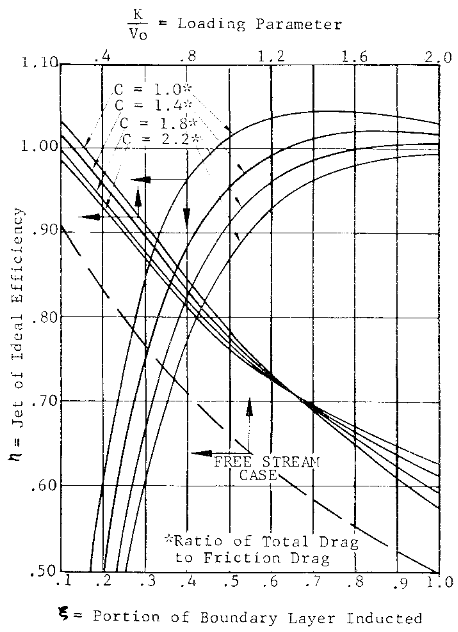

Fig. 6 Effects of performance parameters on ideal efficiency for a propulsor inducting the boundary layer on a body of revolution for $n = 7$.

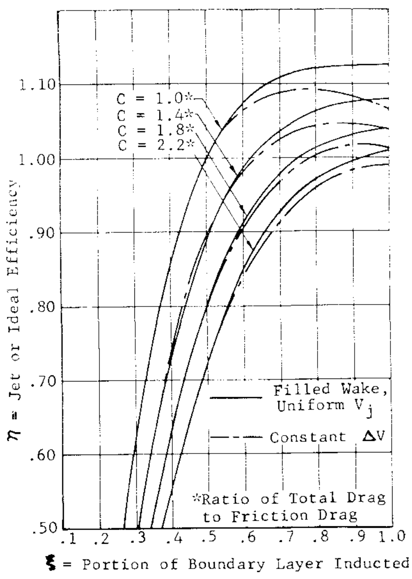

Fig. 8 Effects of performance parameters on ideal efficiency for a propulsor inducting the boundary layer on a body of revolution for $n = 3$.

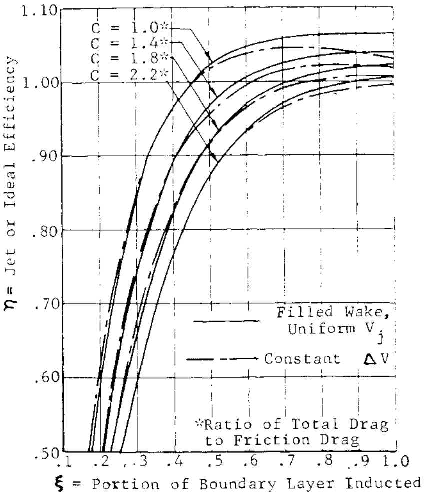

Fig. 9 Effects of performance parameters on ideal efficiency for a propulsor inducting the boundary layer on a body of revolution for $n = 7$.

value of the analysis since the loading parameter was an implicit function of the more pertinent parameters.

As the wake is now completely filled, the attainable efficiencies are higher. However, Fig. 7, which shows the maximum attainable jet efficiency as a function of the exponent n for various values of C, illustrates that the loading parameter does not have a strong influence. Reference 1 reported the same result. This is of direct interest, as the implication is that the present results would be applicable in general to cases of loading parameters which deviate from those presented herein to some extent.

Comparison with Experiment

The spectrum of parameters influencing the jet efficiency over a wide range has been defined. It is important, now, to determine how that spectrum applies in specific cases involving typical underwater bodies, and in general to substantiate the analysis by means of experimental results. Therefore, a brief survey of the literature was made to find experimental results. Although a number of reports and papers of direct interest were found the results, in many cases, were incomplete and not directly comparable. Also, the literature search for experimental results was limited to unclassified information. However, several pertinent reports were found and are discussed subsequently.

Reference 3 presents a complete discussion of torpedo propellers. Detailed velocity distributions measured at the plane

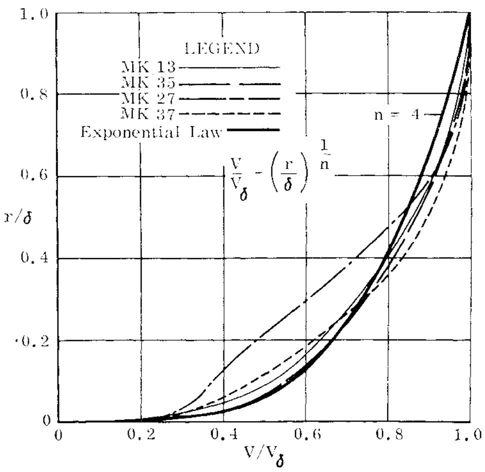

Fig. 10 Velocity profiles at propeller station of several torpedoes.

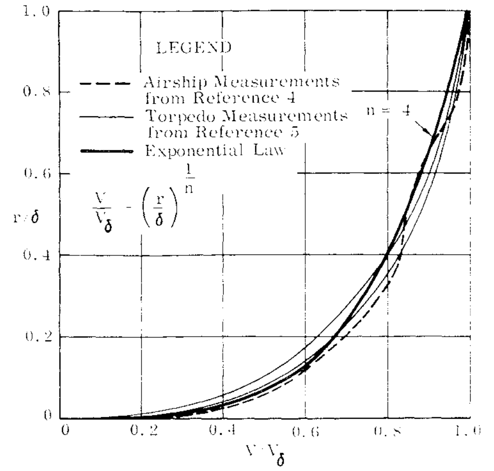

Fig. 11 Velocity profiles at propeller station of airship model and research torpedo.

of the propeller are shown for four different torpedoes. In addition, the performance of several different propellers on a model MK-13 torpedo are experimentally determined. Reference 4 presents similar measurements on an airship, including detailed velocity profiles and propeller performance, and Ref. 5 presents wind-tunnel test measurements on a model torpedo. Reference 6 presents measurements of turbulent boundary-layer mean velocity distributions with adverse pressure gradients and an associated relation for prediction thereof in terms of boundary-layer parameters.

The first step was to verify the validity of the use of the exponential law to define the boundary layer in the region of an adverse pressure gradient and to determine the approximate range of values of the exponent n for a typical underwater body of revolution. The experimental data presented in Ref. 3–6 provided the basis for these determinations.

The velocity profiles for four different torpedoes are shown in Fig. 10.[3] The data are plotted in terms of V/V_δ as a function of r/δ. These measurements were made on the respective torpedo bodies without the influence of the propeller (no induced effects). The torpedoes vary in length and diameter and to some extent have variations in shape; consistent trends with parameters such as length/diameter were expected, but were not shown by the data. However, the exponential relationship $V = V_\delta(r/\delta)^{1/n}$ shows good correlation with the measurements.

Similar velocity profile measurements for an airship are shown in Fig. 11. Measurements were made at two different circumferential positions at the propeller plane. The effects of the fins were pronounced and produced local anomalies. The average of these two measurements is shown as the representative conditions. Again, the exponential relationship $V = V_\delta(r/\delta)^{1/n}$ shows good correlation. Velocity profiles measured in wind-tunnel tests of an unpowered torpedo model are also shown in Fig. 11. It is of interest that, for both the torpedo and the airship, the exponential relationship where $n = 4$ typifies the average boundary-layer velocity profile at the plane of the propeller.

Other results are available in Ref. 6 which give a more complete picture of the boundary-layer velocity profile for

Table 1 Analytically determined efficiencies for underwater body of revolution

n	Energy addition	Ideal efficiency for $C = 1$	Propeller efficiency based on $\eta_{hyd} = 0.95$
4	Constant ΔV	1.07	1.02
4	Filled wake	1.10	1.05

Table 2 Experimental data of propeller performance

Source	Propellers	Body	Experimental propeller efficiency	Experimental propulsive efficiency	Jet efficiency predicted from analysis	Propeller efficiency pred. from anal. based on $\eta_{hyd} = 0.95$	Propulsive efficiency predicted with $\tau = 0.075$
Ref. 3	MK 13	MK 13 torpedo	1.14	...	1.07–1.10	1.02–1.05	0.95–0.98
	2010	MK 13 torpedo	1.16	...	1.07–1.10	...	...
	Schoenherr	MK 13 torpedo	1.24	...	...	...	...
Ref 4	Experimental	Airship	...	1.03	...	...	...

various adverse pressure gradients. The reference utilizes experimental results from several other sources. The pertinent velocity profile measurements are shown in Fig. 12 with the exponential power law, which fits each curve. Again, the exponential power law shows good correlation. As separation is approached, the exponent n decreases and the expected inflection point in the velocity profile becomes apparent. At separation, the experimentally determined n is approximately equal to 1.22. Therefore, the foregoing measurements on the torpedo and airship illustrate that the flow at the plane of the propeller is not near separation.

The foregoing discussions have established that the exponential power law provides a good representation of the velocity profile at the plane of the propeller, for a typical underwater body of revolution or torpedo. Further, a value of $n = 4$ is indicated from experiment as a good representative value.

The next step is to probe into the efficiencies that can be attained for a typical underwater body of revolution and compare with experiment. Table 1 compends the analysis. The propeller efficiency can be derived if the hydraulic efficiency is known. This can be determined from detailed analysis of the blade element performance and associated losses. This efficiency is dependent on a number of design parameters such as advance ratio, diameter, hub-tip ratio, loading or circulation distribution, and structural and cavitation limitations. Tradeoff of these parameters on a generalized basis is beyond the scope of this article. However, it is reasonable to expect a hydraulic efficiency of 95% for a good present state-of-art design axial flow pump or marine propeller. The propeller efficiency is derived from the jet efficiency by $\eta_{prop} = \eta_{jet} \times \eta_{hyd}$. The propeller efficiency for a typical case is shown in Table 1.

The final step is to determine the propulsive efficiency. This implies that the thrust deduction must be accounted for as follows:

$$\eta_{propul} = \eta_{prop}/(1 + \tau)$$

For a typical torpedo, using a conventional free propeller, $\tau = 0.075$.[3]

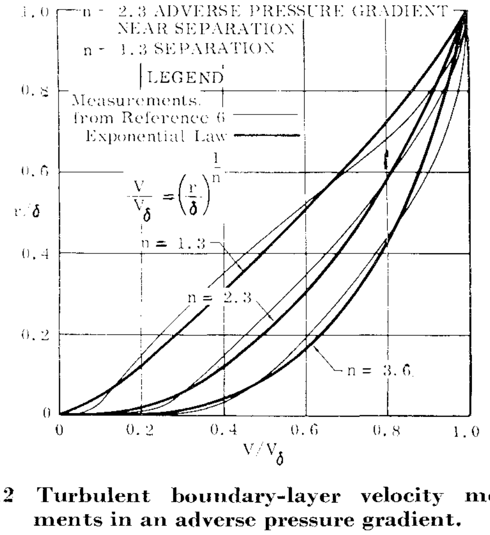

Fig. 12 Turbulent boundary-layer velocity measurements in an adverse pressure gradient.

References 3 and 4 both present experimental data of propeller performance. These are shown in Table 2 and are compared with the typical predicted values from the analysis. Experimental results that were questionable or incomplete are not shown.

The propeller efficiencies presented in Ref. 3 vary from 1.14 to 1.24 as compared with predicted jet efficiencies of 1.07 to 1.10 and propeller efficiencies of 1.02 to 1.05. From Ref. 4, a value of propulsive efficiency of 1.03 is reported, as compared with a predicted value of 0.95 to 0.98. The experimental results are not completely consistent among themselves and, in general, are higher than the predicted results. The largest divergence between predicted and experimental results is present in the torpedo data, whereas relatively good correlation is obtained with the airship data. The reasons for the divergence are not apparent because of the limited data. Additional experimental information is needed.

In order to understand the implication of the analysis and the meaning of efficiencies in the region of or over 100%, the efficiency definition must be reiterated. The efficiency definitions are based on a relationship of energies. For the wake-adapted or boundary-layer propulsor, some of the momentum decrement represented in the boundary layer is recovered and credited to the propulsor. By inducting the major portions of the boundary layer, a large portion of this energy can be recovered and the jet or ideal efficiency can exceed 100%. The theoretical limit on this basis is 200%. In contrast, for the freestream case, a value of 100% represents a theoretical limit. The gross inadequacies of the present definition of propulsive efficiency, as applied to a propulsor inducting boundary-layer fluid, is apparent when it is realized that an efficiency in the absolute sense cannot exceed 100%. However, these high values must be considered in comparing performance with the freestream case.

References

[1] Bevin, V. F. and Miniovich, J. J., "Experimental investigations of interaction between hull and cavitating propeller," 10th International Towing Tank Conference, Teddington, England (1963).

[2] Nelson, D. M., "The effect of propeller cavitation on thrust deduction, a theoretical examination," Bureau of Naval Weapons NAVWEPS Rept. 8549 (September 1964).

[3] McCormick, B. W., Eisenhuth, J. J., and Lynn, J. E., "A study of torpedo propellers," Ordnance Research Lab., Ser. NORD 16597-5, Pt I (March 1956).

[4] McLemore, H. C., "Wind tunnel tests of a $\frac{1}{20}$ scale airship model with stern propellers," NASA TN D-1026 (January 1962).

[5] Hill, F. J., "Wind-tunnel tests of an unpowered model of a research torpedo configuration," Naval Ordnance Lab. NAVORD Rept. 5428 (February 1957).

[6] Sandborn, V. A., "An equation for the mean velocity distribution of boundary layers," NASA Memo. 2-5-59E (February 1959).

[7] Thurston, S. and Vanden Eyckel, E. E., "Hydrodynamic design of the axial flow pumpjet for the torpedo MK 41-Mod 1," Naval Ordnance Test Station Tech. Memo. 645 (June 1952); confidential.

[8] Thurston, S. and Amsler, R., "A review of marine propulsive devices," AIAA Preprint 65-482 (July 1965); also "Review of marine propellers and ducted propeller propulsive devices," J. Aircraft **3**, 255–261 (1966).

[9] Wislicenus, G. F., "Hydrodynamics and propulsion of submerged bodies," ARS J., **30**, 1140–1148 (1960).